Mechanism of the formation of engineered magnesite: A useful mineral to mitigate CO_2 industrial emissions

German Montes-Hernandez[a] *, Mamadou Bah[a], François Renard[a,b]

[a] Univ. Grenoble Alpes, Univ. Savoie Mont Blanc, CNRS, IRD, IFSTTAR, ISTerre, 38000 Grenoble, France

[b] The Njord Centre, PGP, Department of Geosciences, University of Oslo, box 1048 Blindern, 0316 Oslo, Norway

*Corresponding author: G. Montes-Hernandez

E-mail address: german.montes-hernandez@univ-grenoble-alpes.fr

Abstract

Magnesium carbonate production at the industrial scale is a realistic option to reduce the industrial emissions of CO_2. Ultrabasic rocks and/or alkaline mine waste provide magnesium sources and are widely available in the Earth's crust. Here, we investigated the aqueous carbonation of magnesium hydroxide under moderate temperature (25-90°C) and pressure (initial pressure of CO_2=50 bar) using NaOH as the CO_2 sequestering agent. From time-resolved Raman measurements, we demonstrate that the aqueous carbonation of magnesium hydroxide can be an effective engineered method to trap CO_2 into a solid material and produce large amounts of magnesite $MgCO_3$ (6 kg/m^{3}h), or hydromagnesite $Mg_5(CO_3)_4(OH)_2.4H_2O$ (120 kg/m^{3}h) at 90°C or nesquehonite $MgCO_3.3H_2O$ (40 kg/m^{3}h) at 25°C. Higher production rates were measured for nesquehonite (at 25°C) and hydromagnesite (at 60 and 90°C). However, only the magnesite produced at 90°C ensures a permanent CO_2 storage because this mineral is the most stable Mg carbonate under Earth surface conditions, and it could be co-used as construction material in roadbeds, bricks with fire-retarding property and granular fill. The use of specific organic additives can reduce the reaction temperature to precipitate magnesite. For example, ferric EDTA (ethylenediaminetetraacetic acid**)** reduces the temperature from 90 to 60°C. However, more time is required to complete magnesite precipitation reaction at this lower temperature (15h at 90°C and 7 days at 60°C). These results suggests that functionalized organic groups can reduce the energetic barriers during mineral nucleation.

Keywords: Engineered Magnesite Precipitation; Time-Resolved Raman Spectroscopy; Carbon Dioxide Mineralization; CO_2 Mitigation; Mineral Nucleation and Growth

Table of Contents Graphic

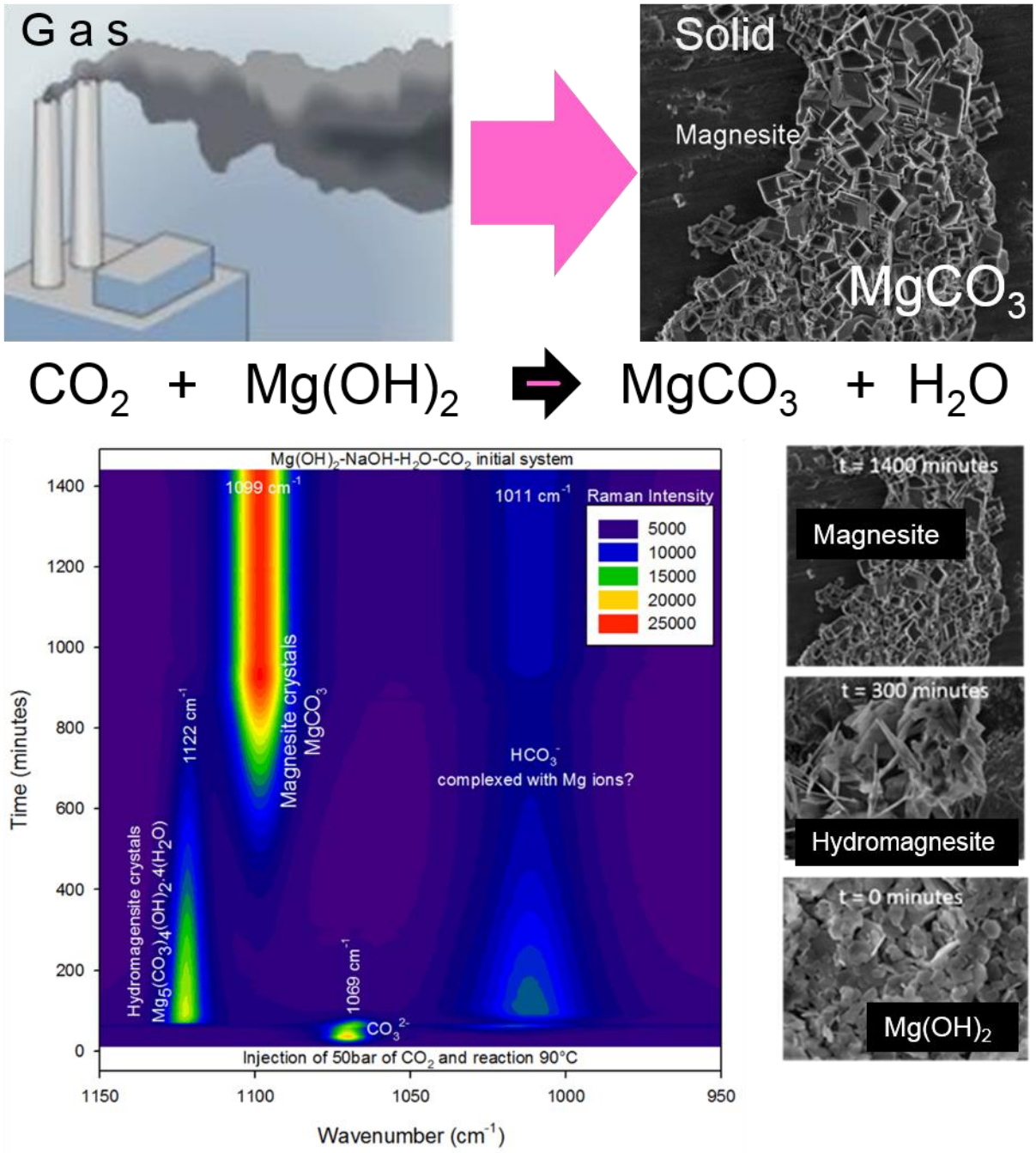

1. Introduction

CO_2 emissions have increased since the industrial revolution: about 36 Gt of CO_2 that originate from fossil fuel are annually emitted into the atmosphere with 30% from industrial activities and 70% from transport, agriculture and other sources [1]. These non-regulated emissions have led to concerns about global warming as a progressive increase of CO_2 concentration into atmosphere has been recorded in the last two centuries [1]. The energy transition (i.e., the use of carbon-free energy sources such as hydrogen, solar, wind, marine, hydraulic, geothermal) could significantly decrease CO_2 emissions. Some limitations, such as the supply of rare Earth elements, large amounts of water requirements and natural risks, have raised some concerns about how fast this transition will occur [2-3]. Moreover, conventional and unconventional fossil resources (gas, carbon and oil) are still available in geological formations [4], and their exploitation and resulting CO_2 emissions have been predicted to continue for 50-100 years [5]. Therefore, CO_2 capture from industrial sources and its transformation into re-usable products (e.g. ethanol, syngas, etc.) and/or non-energetic materials (e.g. calcite, magnesite, siderite, etc.) has been proposed to reduce CO_2 emissions into the atmosphere [6-9]. CO_2 capture from industrial sources does not represent a technological or scientific obstacle, but the existing methods and technologies (including recovery of high-purity of CO_2 and its liquefaction) remain highly expensive. In this way, the improvement and optimization on the CO_2 capture units still represent important challenges. The goal of the present experimental study is to demonstrate that engineered magnesite ($MgCO_3$) could be used as an effective option to store carbon dioxide within magnesite-rich solids. The obtained magnesite-rich solids could then be used as civil construction materials (e.g. roadbed materials, bricks, granular fill) [10]. Magnesite is the most stable carbonate mineral under typical Earth surface

conditions, with the highest resistance to leaching and weathering [11]. The magnesite dissolution rate is 100-1000 times lower than that of calcite in a wide range of conditions, from ambient temperature to 150°C and pH from 1 to 14 [11]. For this reason, anhydrous magnesium carbonates (magnesite and dolomite) have been considered as relevant minerals to store permanently anthropogenic carbon dioxide. Magnesite and dolomite precipitation kinetics have been widely studied because their abiotic precipitation at ambient temperature (~25°C) is virtually impossible within typical experimental time scales [12-13]. The strong solvation shells of magnesium ions in aqueous media produces this limitation [12]. However, the sole effect of Mg hydration might not be the only factor of inhibition of magnesite and/or dolomite formation. Recent studies claim that a more intrinsic crystallization barrier and the influence of fluid chemistry (e.g., relative size of the constituting cations) prevent the formation of a long-range ordered crystallographic structures at ambient conditions [14-15]. Conversely, a recent study has reported magnesite precipitation in batch reactors at room temperature after 77 days of reaction with the aid of carboxylated polystyrene microspheres [16]. Diluted ionic solutions (<0.1M) and microspheres coated with a high density of carboxyl groups at their surface allowed the binding and dehydration of Mg^{2+} ions in solution, thereby minimizing the kinetic barrier and facilitating magnesite formation [16]. However, the reaction mechanism and the nature of precipitating minerals between 1 and 77 days remain to be identified, and whether precipitation occurred via the formation of transient phases or by a direct nucleation event is unknown. Moreover, this method needs to be up-scaled to produce high-amounts of magnesite in reasonable time (24 hours). In order to overcome these limitations, the present study demonstrates magnesite precipitation at moderate temperature (60 and 90°C) by aqueous carbonation of magnesium hydroxide ($Mg(OH)_2$) under anisobaric conditions (initial CO_2 pressure = 50 bar). These conditions allow the production of high amounts of magnesite in only

15h at 90°C or 7 days at 60°C. Herein, NaOH was used as a CO_2 sequestering agent and the ferric EDTA as a dehydration agent of Mg^{2+} ions. Magnesium hydroxide was chosen because its engineered production from olivine and serpentine-rich materials was actively investigated for CO_2 mineralization purpose [17-18]. Magnesium oxide (MgO) and magnesium hydroxide ($Mg(OH)_2$ may be produced from serpentine and other Mg-rich silicates. Both synthesized minerals have numerous industrial applications, and have been proposed as sinks to store anthropogenic carbon dioxide by transforming it into magnesium carbonate minerals [17-18].

2. Materials and Methods

2.1. Magnesite precipitation using NaOH as sequestering agent of CO_2

As already demonstrated in our group (e.g. [8, 19]), the NaOH enhances the magnesite precipitation at 90°C via aqueous carbonation process of magnesium hydroxide with compressed CO_2. An initial CO_2 pressure of 50bar ensures an excess of CO_2 with respect to $Mg(OH)_2$ in the reactor and ideal gas condition. In the present study, two new experiments were performed at 90 and 27°C, respectively, and monitored by time-resolved in situ Raman spectroscopy as described in Montes-Hernandez and Renard, 2016 [19]. Herein, carbonate speciation and precipitated particles were monitored for 24h with a 1-minute spectral acquisition time. The Raman spectra were treated in order to estimate the position, full wide half maximum (FWHM) and integrated surface area as a function of time for specific stronger peaks in order to explain the reaction mechanism and kinetics of Mg carbonates precipitation and particularly magnesite ($MgCO_3$).

126 *2.2. Magnesite precipitation using NaOH and organic additives*

127 Magnesite precipitation was also investigated at 60°C in the presence of three organic molecules
128 (Aspartame, ferric EDTA, and citric acid tri-sodium salt), expecting a dehydration effect of Mg^{2+}
129 ions or a chelation effect. In these experiments, 15 g of $Mg(OH)_2$, provided by Sigma-Aldrich with
130 chemical purity of 99%, 20g of NaOH, 1 g of organic additive, and 500 mL of high-purity water
131 were mixed in the reactor (total internal volume of 960 mL). The slurry was immediately dispersed
132 by mechanical agitation (400 rpm) and gaseous CO_2, provided by Linde Gas S.A., was injected at
133 50 bar into the reactor. About 3 minutes at 25°C were required to reach the pre-defined pressure.
134 The agitation speed was kept to 400 rpm using a rotor with two blades (Parr reactor) that ensured
135 homogeneous dispersion of reacting and precipitating solids and fast dispersion of the injected CO_2
136 in the system. Following injection, the system was heated to 60°C, the pH of the solution and the
137 CO_2 consumption (pressure drop) were monitored in-situ during mineral formation for 24, 72 or
138 168 hours.

139 At the end of the experiment, the residual CO_2 was degassed from the reactor by opening the gas
140 line valve for five minutes. The solid product was recovered by centrifugation and washed twice
141 with ultrapure water and then was dried directly in the centrifugation flasks at 60 °C for 48 h. The
142 dry solid products were stored in plastic flasks for subsequent characterization by Raman
143 spectroscopy, Field Emission Gun Scanning Electron Microscopy (FESEM) and powder X-ray
144 diffraction (XRD). All ten performed experiments are summarized in Table 1.

145

146

147 *2.3. Ex situ characterization of precipitates*

148 XRD analyses were performed using a Siemens D5000 diffractometer in Bragg-Brentano
149 geometry, equipped with a theta-theta goniometer with a rotating sample holder. Diffraction
150 patterns were collected using Cu $k\alpha_1$ ($\lambda_{k\alpha1}$=1.5406 Å) and $k\alpha_2$ ($\lambda_{k\alpha2}$=1.5444 Å) radiation in the
151 range 2θ = 10 - 70°, with a step size of 0.04° and a counting time of 6 seconds per step. For high-
152 resolution imaging, the solid products were dispersed by ultrasonic treatment in absolute ethanol
153 for five to ten minutes. One or two droplets of the suspension were then deposited directly on an
154 aluminum support and coated with platinum. The morphology of the crystals was imaged using a
155 Zeiss Ultra 55 FESEM with a maximum spatial resolution of approximately 1 nm at 15kV.

156 *2.4. Calculation of production rate*

157 The production rate of a given magnesium carbonate was calculated as follows:

158 $P_{rate} = (\lambda * Mol_{Mg(OH)2} * M_{MgCarbonate})/(t_{max} * V_{reactor})$

159 where λ is the chemical conversion factor for Mg carbonate phases determined from Raman
160 spectroscopy when peaks intensity is constant for a given time-interval. The value λ=1 is reached
161 when the peak intensity for a given Mg carbonate is constant and only a single mineral is detected.
162 $Mol_{Mg(OH)2}$ is the initial amount (in mol) of $Mg(OH)_2$ (complete transformation was determined
163 from ex-situ XRD measurements in recovered solid products); $M_{MgCarbonate}$ is the molar mass of a
164 given Mg carbonate; t_{max} is the time where only one mineral phase exists and the peak intensity is
165 constant; $V_{reactor}$ is the effective volume of the reactor which is equal to0.6L (runs 1-2) or 1L (runs
166 3-10). This calculation using time-resolved experimental measurements could allow a realistic
167 extrapolation to pilot and/or industrial scale assuming roughly proportional dimensions and

168 equivalent precipitation times.

169

170 **3. Results and discussion**

171 *3.1. Magnesite precipitation at 90°C: Reaction mechanism and kinetics*

172 Carbonation of $Mg(OH)_2$ at 25°C leads the precipitation of nesquehonite, with the following global
173 reaction:

174 $Mg(OH)_2 + CO_2 + 2H_2O \rightarrow MgCO_3 \cdot 3H_2O$ (1)

175 The successive events involved during magnesium hydroxide carbonation are displayed in Fig. 1.
176 Dissolved NaOH enhanced the rate and amount of sequestration of injected CO_2 (initial P_{CO2} =50
177 bar). The carbon dioxide dissolved into interacting alkaline solution ($CO_{2(gas)} \leftrightarrow CO_{2(aq)}$) was
178 rapidly dissociated into CO_3^{2-} ($CO_{2(aq)} + 2NaOH \rightarrow CO_3^{-2} + H_2O + 2Na^+$). A fraction of the
179 carbonate ions was protonated after about 60 minutes ($CO_3^{-2} + H^+ \rightarrow HCO_3^-$) producing a pH change
180 in the interacting solution, and simultaneously enhancing the dissolution of magnesium hydroxide
181 ($Mg(OH)_2 \rightarrow Mg^{2+} + 2OH^-$). All these combined reactions led to the precipitation of nesquehonite
182 ($Mg^{2+} + HCO_3^- + 3H_2O \rightarrow MgCO_3.3H_2O + H^+$) with a nucleation induction time of 105 minutes.
183 This mineral grew by continuous dissolution of magnesium hydroxide until complete consumption
184 in the reactor. Nesquehonite remained stable in the interacting solution until the end of experiment
185 (72 h). Ex-situ FESEM images revealed micrometric crystals of prismatic elongated morphology
186 (Fig. SI-1). Time-resolved Raman measurements and ex-situ characterization of solid confirm that
187 magnesite precipitation was inhibited by nesquehonite precipitation at 25°C. Conversely,
188 magnesite formation was rapidly obtained at 90°C and only 15 h were required to produce high-
189 purity magnesite (~6 kg/m^3h) as monitored by Raman spectroscopy (Fig. 2). The global reaction

summarizes the process:

$Mg(OH)_2 + CO_2 \rightarrow MgCO_3 + H_2O$ (2)

A complete aqueous carbonation reaction was obtained at 90°C exclusively when NaOH was used as the CO_2 sequestering agent, in agreement with previous results [8]. In the present study, a more detailed reaction mechanism and kinetics are demonstrated from the time-resolved in-situ Raman spectroscopy measurements and all temporal reaction events are shown in Fig. 2 and Fig. SI-2. Similar to the nesquehonite case, the aqueous carbon dioxide ($CO_{2(gas)} \leftrightarrow CO_{2(aq)}$) was rapidly dissociated into CO_3^{2-} ($CO_{2(aq)} + 2NaOH \rightarrow CO_3^{-2} + H_2O + 2Na^+$), but this reaction remained active only during the first 100 minutes. Then, carbonate ions were rapidly protonated, forming bicarbonate ions ($CO_3^{-2} + H^+ \rightarrow HCO_3^-$) that may complex with Mg^{2+}, leading to a shift of the maximum of the Raman peak of HCO_3^- from 1020 cm^{-1} (Fig.1) to 1011 cm^{-1} (Fig. 2). After 150 minutes, aqueous carbon dioxide and bicarbonate ions were the dominant species in the reactor, which induced a significant pH change in the interacting solution as suggested from carbonate speciation in relation with pH (inorganic carbonate fraction vs pH diagram). Under these conditions, the dissolution of magnesium hydroxide ($Mg(OH)_2 \rightarrow Mg^{2+} + 2OH^-$) was enhanced, and the release of magnesium ions generated oversaturation states with respect to several magnesium carbonates. Consequently, the nucleation of hydromagnesite was detected in-situ after 60 minutes of reaction (first nucleation-event).

$5Mg^{2+} + 4HCO_3^- + 6H_2O \rightarrow Mg_5(CO_3)_4(OH)_2.4H_2O + 6H^+$ (3)

Hydromagnesite formed as a transient mineral phase that reached a maximum spectral intensity after 120 minutes. Then, this mineral dissolved in a destabilization processes through a decrease of spectral peak surface area (i.e., Fig. 3) progressively before the nucleation of magnesite that was detected after 240 minutes of reaction (second nucleation-event).

213 $Mg^{2+} + HCO_3^- \rightarrow MgCO_3 + H^+$ (Nucleation) (4)

214 After this magnesite nucleation event, the growth of magnesite was mainly nourished by
215 progressive dissolution of hydromagnesite. The temporal evolution of peak surface areas and Full
216 Width Half Maximum (FWHM) for hydromagnesite and magnesite minerals (Figs. 3 and 4)
217 suggest that this reaction included coupled dissolution-reprecipitation. Hydromagnesite was
218 completely consumed after 13 h. An Ostwald repining process could explain the growth in the
219 following two hours. Equilibrium was reached after 15 h of reaction, as demonstrated by the
220 constant FWHM of magnesite after this time (Fig. 4). FESEM images revealed rhombohedral
221 single crystals with sizes <5 μm (Fig. SI-3), in agreement with previous work [8].

222

223 *3.2. Role of temperature and organic additives*

224 Several complementary experiments were performed in order to assess the evolution of pH in-situ,
225 the dehydration effect of organic additives around Mg ions, and the role of reaction temperature
226 (Table 1, Fig. 5). For all of these experiments, the pH decreased from 12.4 to 9 in the first 10
227 minutes and then continued to decrease at a slower rate until stabilization to a value in the range
228 5.5-6 after 1 h of reaction. This result indicates that the pH was mainly controlled by inorganic
229 carbonate speciation and CO_2 pressure (Figs. SI-4 and 5), and that organic additives had a little or
230 undetected influence. This result is in agreement with time-lapse Raman measurements where a
231 protonation process of carbonate ions was also detected, indicating a pH change in the interacting
232 solution (Figs. 1, 2). Conversely, organic additive has significant effect on the texture (crystal size)
233 and structural water content of the mineral produced, as identified in recovered suspensions by
234 Raman ex-situ measurements (Fig. 5). Hydromagnesite was the main mineral phase precipitated at
235 60°C for 24 h in the absence or presence of organic additive. However, both the mineral texture,

236 measured by the Full Width Half Maximum (FWHM) of the largest Raman peak, and the structural
237 water content, measured by the position of largest Raman peak, were slightly different with respect
238 to the reference of the hydromagnesite precipitated in a solution free of additive. In addition, some
239 traces of magnesite were detected after 24 h of reaction when ferric EDTA or citric acid tri-sodium
240 salt were used. For the EDTA additive, slow hydromagnesite-to-magnesite transformation was
241 detected and about 7 days were required to obtain high-purity magnesite at 60°C. Only
242 nesquehonite was detected at 25°C in the presence of EDTA (Fig. 5). This result confirms that
243 magnesite precipitation from the aqueous carbonation of magnesium hydroxide at room
244 temperature was inhibited, or strongly retarded, by the precipitation of nesquehonite.
245
246 *3.3 Environmental implications*
247 Magnesite formation at room temperature (<30°C) from the aqueous carbonation of magnesium
248 hydroxide remains a scientific challenge. This formation could make the magnesite precipitation
249 an economical issue to store permanently the CO_2 with important environmental advantages:
250 (1) reduce CO_2 emissions from the industrial sector (e.g. steel and cement industry, coal-fired
251 power),
252 (2) obtain magnesite-rich or high-purity magnesite materials with an aggregate value (e.g.
253 fabrication of roadbed materials, bricks, granular fill, fire-retardant building material) at low or
254 moderate temperature and reduced time (<24 h) and,
255 (3) use of mine solid wastes (e.g., mines in ultrabasic rocks) or widely available Mg-silicates as a
256 magnesium source to capture CO_2.
257 In practice, the residual alkaline-solution used during magnesite production could be recycled for
258 future carbonation experiments or re-used in other chemical processes, but these options were not

assessed in the present study.

In this context, the production of magnesite material as an effective solution to reduce the industrial CO_2 emission may be a serious option at industrial scale as now proposed by Cambridge Carbon Capture (http://www.cacaca.co.uk/#news).

4. Conclusion

In the present study, we demonstrated that high-purity magnesite can be produced from the carbonation of magnesium hydroxide at a rate of about 6 kg/m^3h, and thus a mineralization rate of CO_2 into magnesite of about $3kg/m^3h$. Higher productions were estimated for hydromagnesite (120 kg/m^3h) and nesquehonite (40 kg/m^3h), but these minerals are thermodynamically less stable at Earth surface conditions than magnesite.

Our time-resolved Raman measurements allowed a detailed description of reaction mechanism and kinetics of carbonation of magnesium hydroxide in batch reactor conditions. This experimental setup offers new possibilities for investigating mineral condensation from ionic solutions and slurries, and for investigating other chemical reactions at the solid-fluid interfaces.

Acknowledgements

The authors acknowledge funding from the French National Centre for Scientific Research (CNRS). We thank Nathaniel Findling for technical assistance.

References

[1] Peters et al. Towards real time verification of CO2 emissions Nature Climate Change 7 (2017) 848-850. https://doi.org/10.1038/s41558-017-0013-9

[2] Montes-Hernandez et al. Mineral sequestration of CO_2 by aqueous carbonation of coal combustion fly-ash, Journal of Hazardous Materials 161 (2009) 1347-1354.

[3] Mediavilla et al. The transition towards renewable energies: Physical limits and temporal conditions. Energy Policy 52 (2013) 297-311.

[4] P. Berg, A. Boland, Analysis of Ultimate Fossil Fuel Reserves and Associated CO_2 Emissions in IPCC Scenarios. Natural Resources Research 23 (2014) 141-158.

[5] G. Montes-Hernandez, F. Renard, R. Lafay, Experimental assessment of CO_2-mineral-toxic ion interactions in a simplified freshwater aquifer: Implications for CO_2 leakage from deep geological storage. Environmental Science & Technology 47 (2013) 6247-6253.

[6] S. Bai, Q. Shao, P. Wang. Q. Dai, X Wang, X. Huang, Highly Active and Selective Hydrogenation of CO_2 to Ethanol by Ordered Pd–Cu Nanoparticles. J. Am. Chem. Soc. 139 (20) (2017) 6827-6830.

[7] M. B. Ross, C. T. Dinh, Y. Li, D. Kim, P. De Luna, E. H. Sargent, P. Yang, Tunable Cu Enrichment Enables Designer Syngas Electrosynthesis from CO_2. J. Am. Chem. Soc. 139 (27) (2017) 9359-9363.

[8] G. Montes-Hernandez, F. Renard, R. Chiriac, N. Findling, F. Toche, Rapid precipitation of magnesite micro-crystals from $Mg(OH)_2$-H_2O-CO_2 slurry enhanced by NaOH and a heat-ageing

step (from ~20 to 90°C). Crystal Growth & Design 12 (2012) 5233-5240.

[9] G. Montes-Hernandez, G. Sarret, R. Hellmann, N. Menguy, D. Testemale, L. Charlet, F. Renard, Nanostructured calcite precipitated under hydrothermal conditions in the presence of organic and inorganic selenium. Chemical Geology 290 (2011) 109-120.

[10] National Academies of Sciences, Engineering, and Medicine. 2019. *Gaseous Carbon Waste Streams Utilization: Status and Research Needs*. Washington, DC: The National Academies Press. https://doi.org/10.17226/25232.

[11] O. S. Pokrovski, S. V. Golubev, J. Schott, A. Castillo, Calcite, dolomite and magnesite dissolution kinetics in aqueous solutions at acid to circumneutral pH, 25 to 150 C and 1 to 55 atm pCO_2: New constraints on CO_2 sequestration in sedimentary basins. Chem. Geol. 265 (2009) 20-32.

[12] J. C. Deelman, Breaking Ostwald's rule. Chemie Der Erde-Geochemistry 61 (2001) 224-235.

[13] C. Pimentel, C. M. Pina, The formation of the dolomite-analogue norsethite: Reaction pathway and cation ordering. Geochim. Cosmochim. Acta 142 (2014) 217-223.

[14] M. Hänchen, V. Prigiobbe, R. Baciocchi, M. Mazzotti, Precipitation in the Mg-carbonate system-effects of temperature and CO2 pressure. Chem. Eng. Sci. 63 (2008) 1012-1028.

[15] J. Xu, C. Yan, F. Zhang, H. Konishi, H.; Xu, H. Teng, Testing the cation-hydration effect on the crystallization of Ca-Mg-CO3 systems. Proc. Natl. Acad. Sci. 2013 doi: 10.1073/pnas.1307612110.

[16] I. M. Power, P. A. Kenward, G. M. Dipple, M. Raudsepp, Room temperature magnesite precipitation. Cryst. Growth Des. 17 (2017) 5652-5659.

[17] E. Nduagu, I. Romao, J. Fagerlund, R. Zevenhoven, Performance assessment of producing $Mg(OH)_2$ for CO_2 mineral sequestration. Applied Energy 106 (2013) 116-126.

[18] S. Madeddu, M. Priestnall, E. Godoy, R. V. Kumar, S. Raymahasay, M. Evans, R. Wang, S. Manenye, H. Kinoshita, Extraction of Mg(OH)2 from Mg silicate minerals with NaOH assisted with H2O: implications for CO2 capture from exhaust flue gas. Faraday Discussions 183 (2015) 369-387.

[19] G. Montes-Hernandez, F. Renard, Time-resolved in situ Raman spectroscopy of the nucleation and growth of siderite, magnesite and calcite and their precursors**.** Crystal Growth & Design 16 (2016) 7218-7230.

354 Table 1. Experiments of magnesium carbonates precipitation from $Mg(OH)_2$-NaOH-H_2O-CO_2
355 slurry under anisobaric conditions (initial CO_2 pressure of 50bar).

Run	Temperature (°C)	Additive (1g)	Real-time monitoring	Exp. Duration (h)	Mineral transient phase(s)	Final mineral phase(s)
1	25	-	Raman spectroscopy	72	none	nesquehonite
2	90	-	Raman spectroscopy	24	hydromagnesite	magnesite
3	90	-	pH probe	24	N/A	Magnesite and residual hydromagnesite
4	60	-	pH probe	24	N/A	hydromagnesite
5	60	citric acid	pH probe	24	N/A	hydromagnesite
6	60	aspartame	pH probe	24	N/A	hydromagnesite
7	60	EDTA	pH probe	24	N/A	hydrogmagnesite
8	60	EDTA	pH probe	72	N/A	magnesite and hydromagnesite
9	60	EDTA	pH probe	168	N/A	magnesite
10	25	EDTA	pH probe	168	N/A	nesquehonite

356

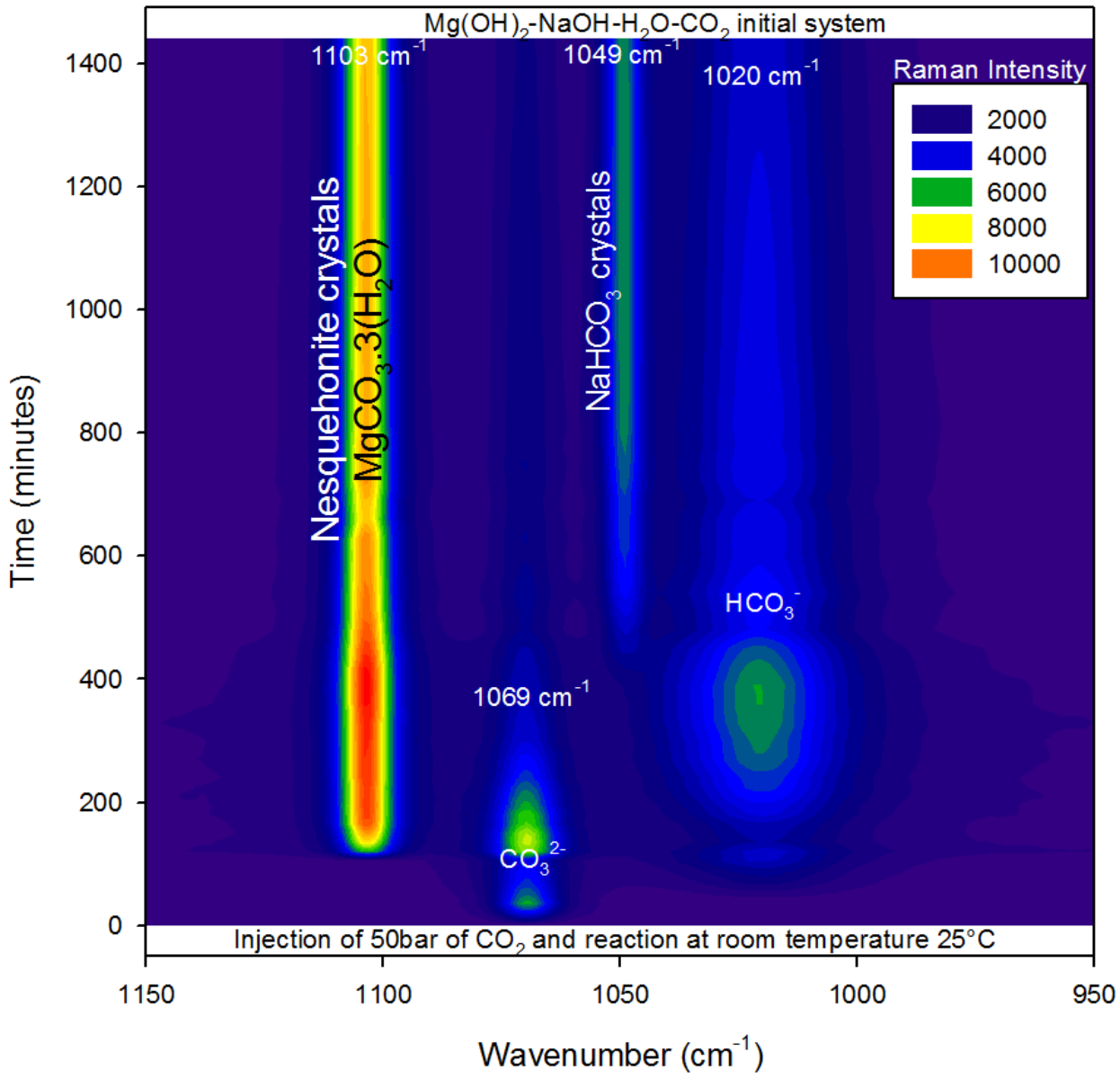

357

358 Figure 1. Time-lapse Raman spectroscopy monitoring of the aqueous carbonation of magnesium
359 hydroxide at 25 °C under anisobaric conditions. The positions of the Raman peaks and the
360 corresponding aqueous or mineral species are indicated on the figure.

361

362

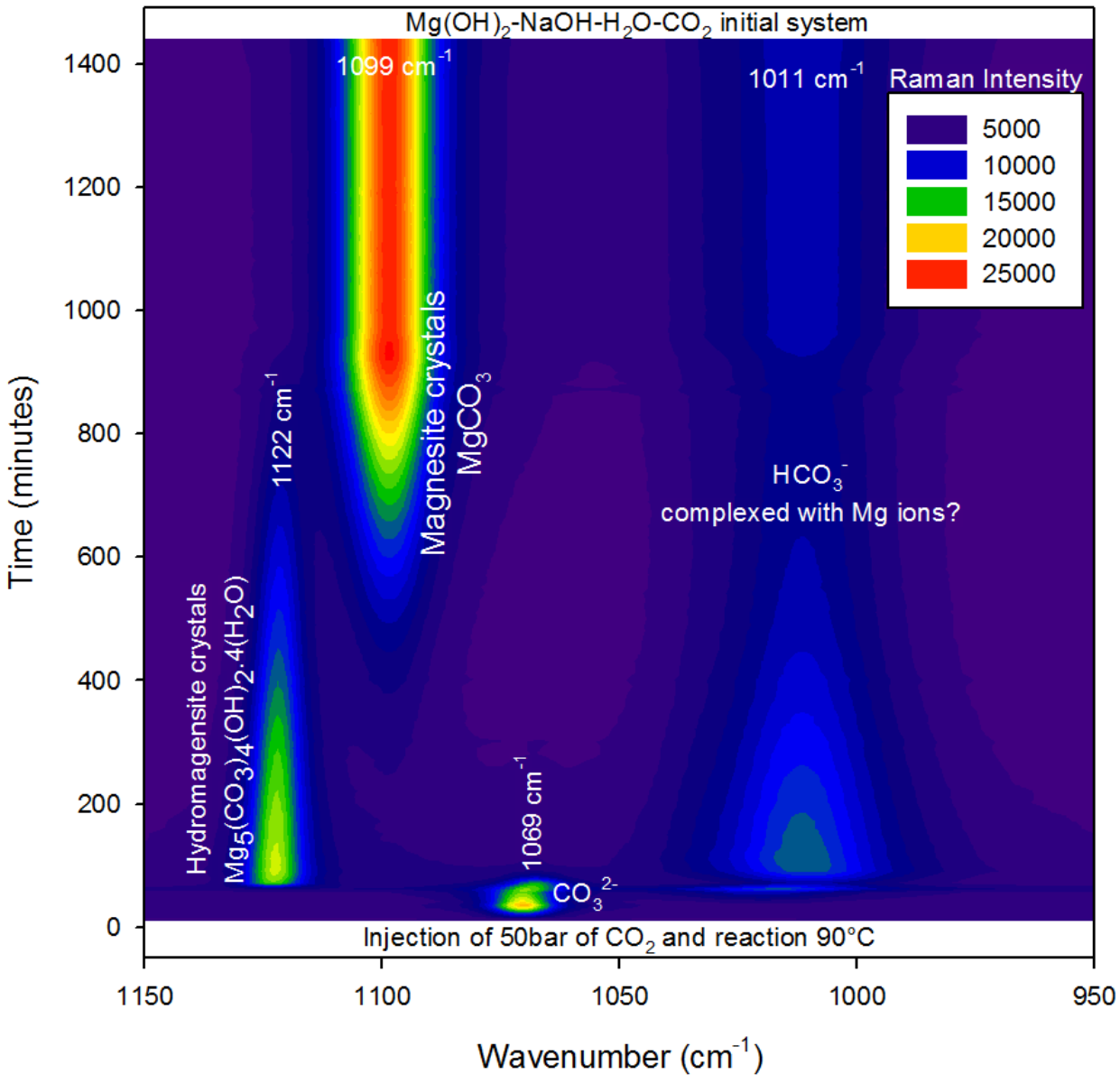

363

364 Figure 2. Time-lapse Raman spectroscopy monitoring of the aqueous carbonation of magnesium
365 hydroxide at 90°C under anisobaric conditions. The positions of the Raman peaks and the
366 corresponding aqueous or mineral species are indicated on the figure. The same data are shown on
367 Fig. SI-2 in the form of spectra.

368

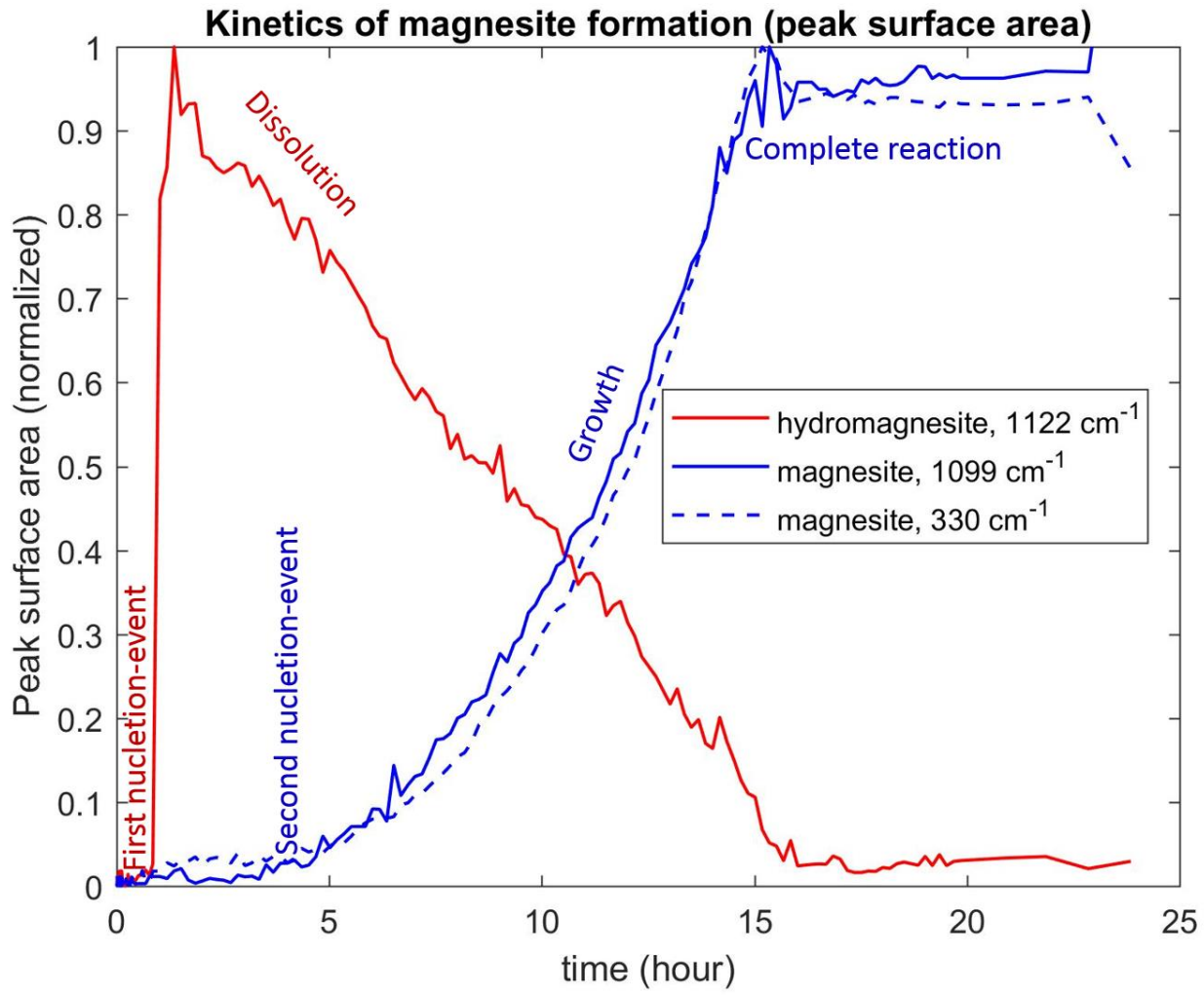

Figure 3. Kinetics of nucleation and growth of hydromagnesite and magnesite during aqueous carbonation of magnesium hydroxide at 90°C measured by Raman spectroscopy. The peak surface area is calculated as a function of time for one Raman peak of hydromagnesite and two Raman peaks for magnesite, from the data shown in Figs. 2 and SI-2.

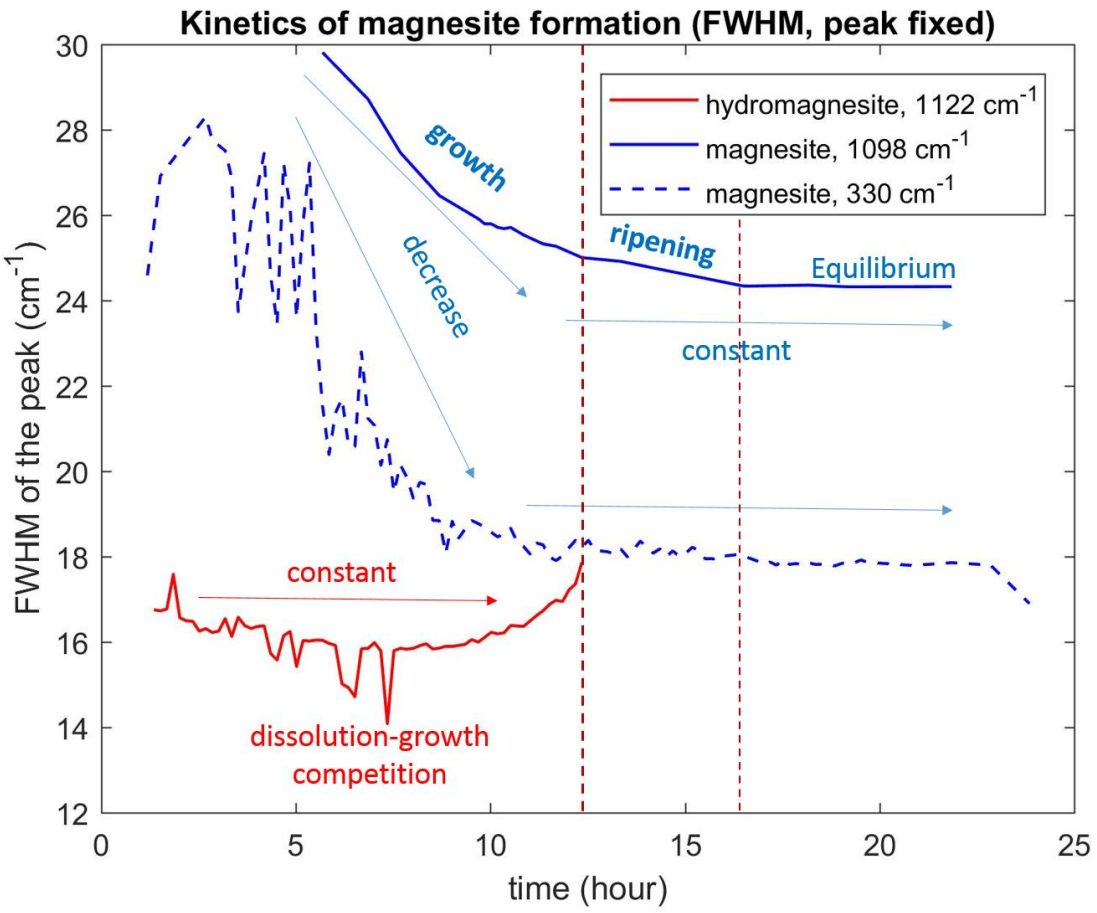

375

376 Figure 4. Crystal growth mechanism of magnesite (blue) at 90°C, nourished by hydromagnesite
377 dissolution (red) and measured by the Full Width at Half Maximum (FWHM) of the Raman peaks
378 shown in Figs. 2 and SI-2.

379

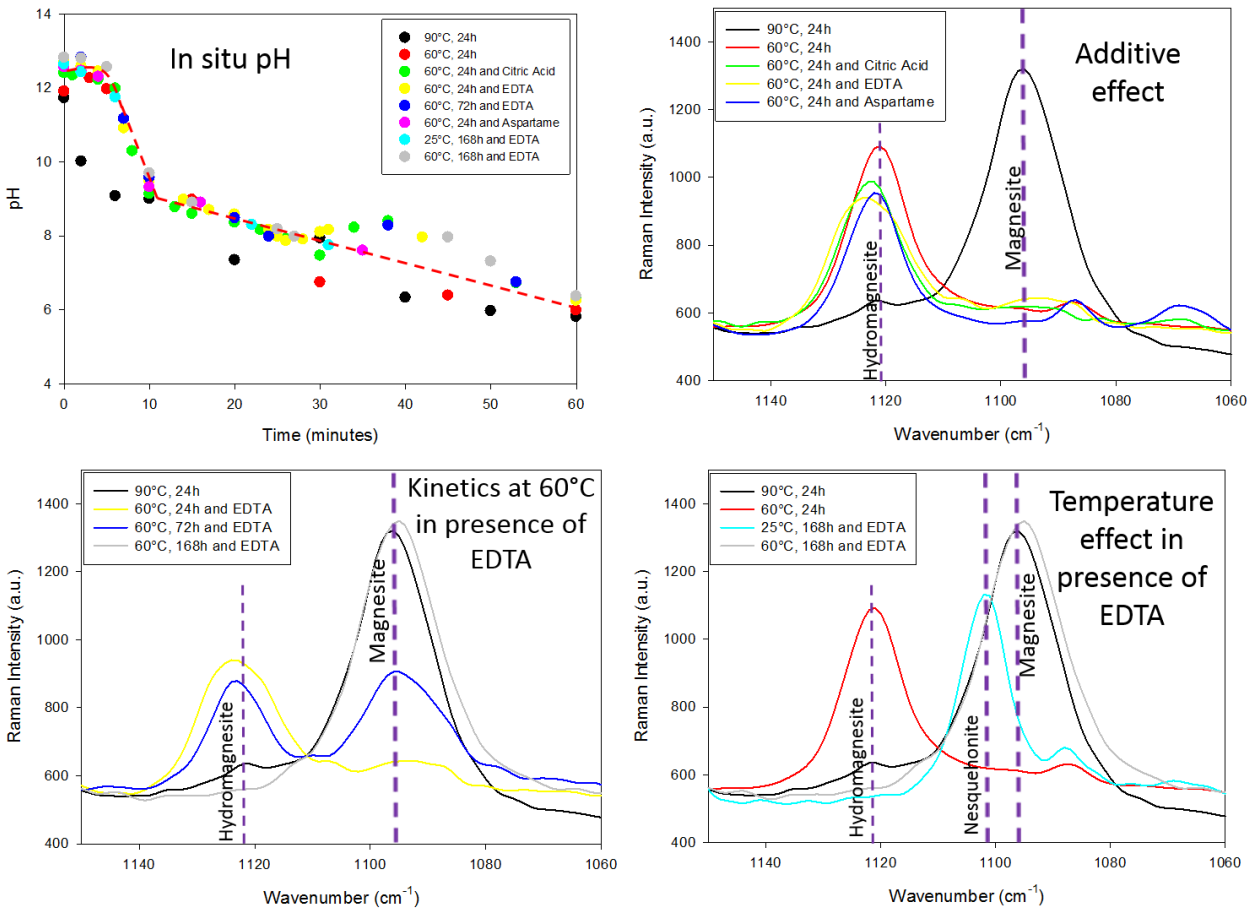

380

381 Figure 5. pH measured in-situ during aqueous carbonation of magnesium hydroxide in eight
382 experiments (Table 1), with or without additive. Influence of organic additives and temperature on
383 the aqueous carbonation of magnesium hydroxide ($Mg(OH)_2$-NaOH-H_2O-CO_2 slurry) under
384 anisobaric conditions.

385

Supporting information

Mechanism of engineered magnesite formation, a useful mineral to mitigate CO_2 industrial emissions

German Montes-Hernandez[a] *, Mamadou Bah[a], François Renard[a,b]

[a] Univ. Grenoble Alpes, Univ. Savoie Mont Blanc, CNRS, IRD, IFSTTAR, ISTerre, 38000 Grenoble, France

[b] The Njord Centre, PGP, Department of Geosciences, University of Oslo, box 1048 Blindern, 0316 Oslo, Norway

*Corresponding author: G. Montes-Hernandez

E-mail address: german.montes-hernandez@univ-grenoble-alpes.fr

The Supporting Information contains three figures, labelled SI-1 to SI-3.

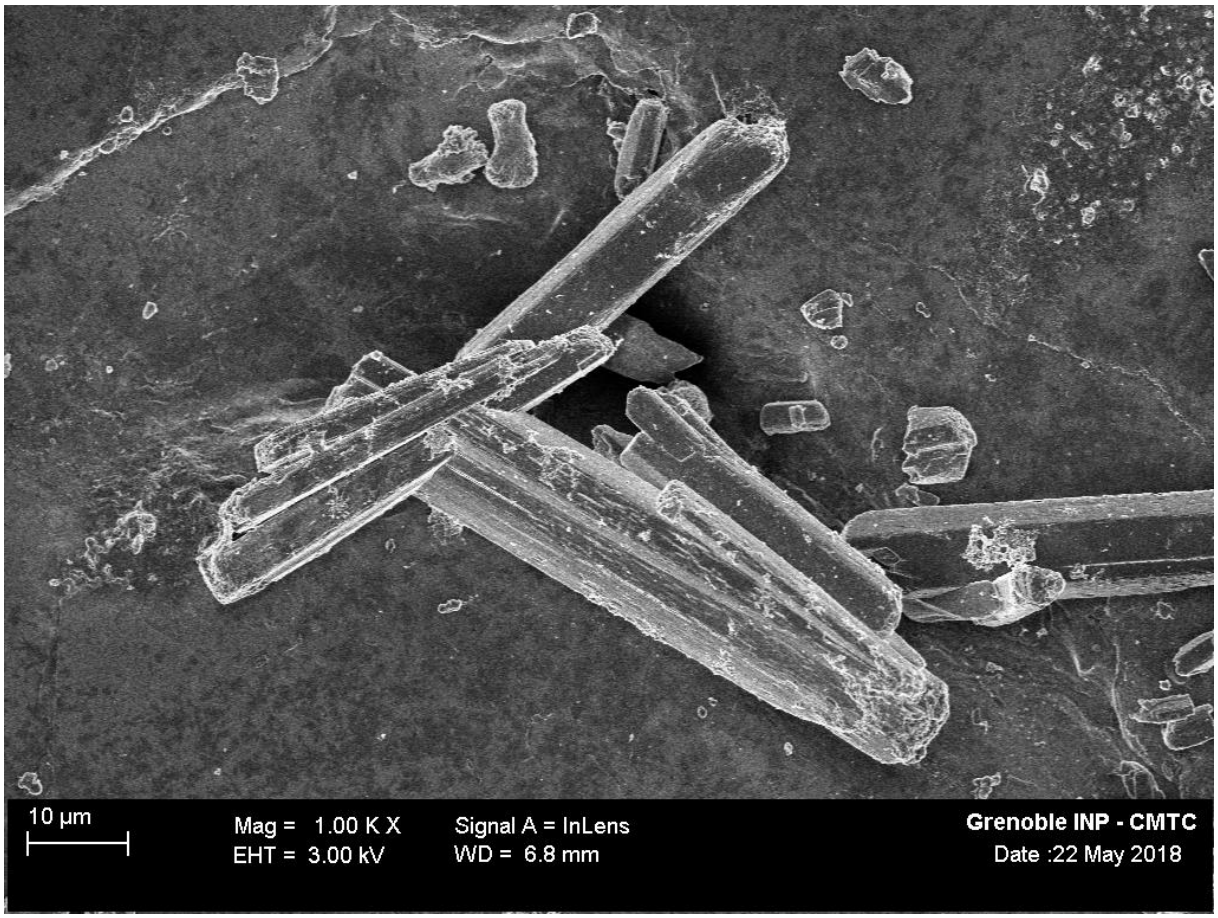

Figure SI-1 Field-emission gun scanning electron microscopy image of nesquehonite crystals with elongated morphology produced after 72h at 25°C (run 1 in Table 1).

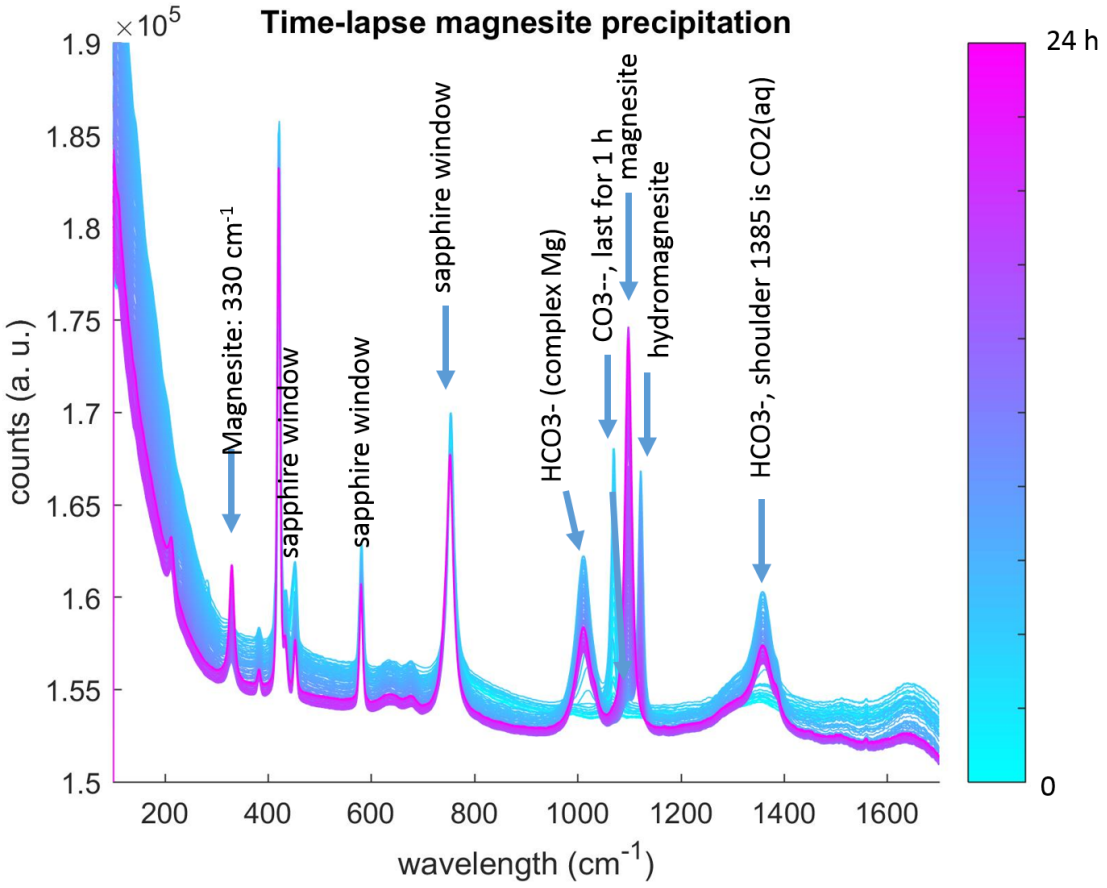

Figure SI-2 Time-lapse Raman spectroscopy monitoring of the aqueous carbonation of magnesium hydroxide at 90°C under anisobaric conditions (run 2 in Table 1). The corresponding aqueous or mineral species are indicated on the figure. The color code indicates time since the beginning of the experiment. The surface area and the full width at middle height (FWMJ) of the peaks of magnesite at 330 cm^{-1} and 1099 cm^{-1} and hydromagnesite at 1122 cm^{-1}, are used to calculate the kinetics curves shown in Figures 3 and 4, respectively.

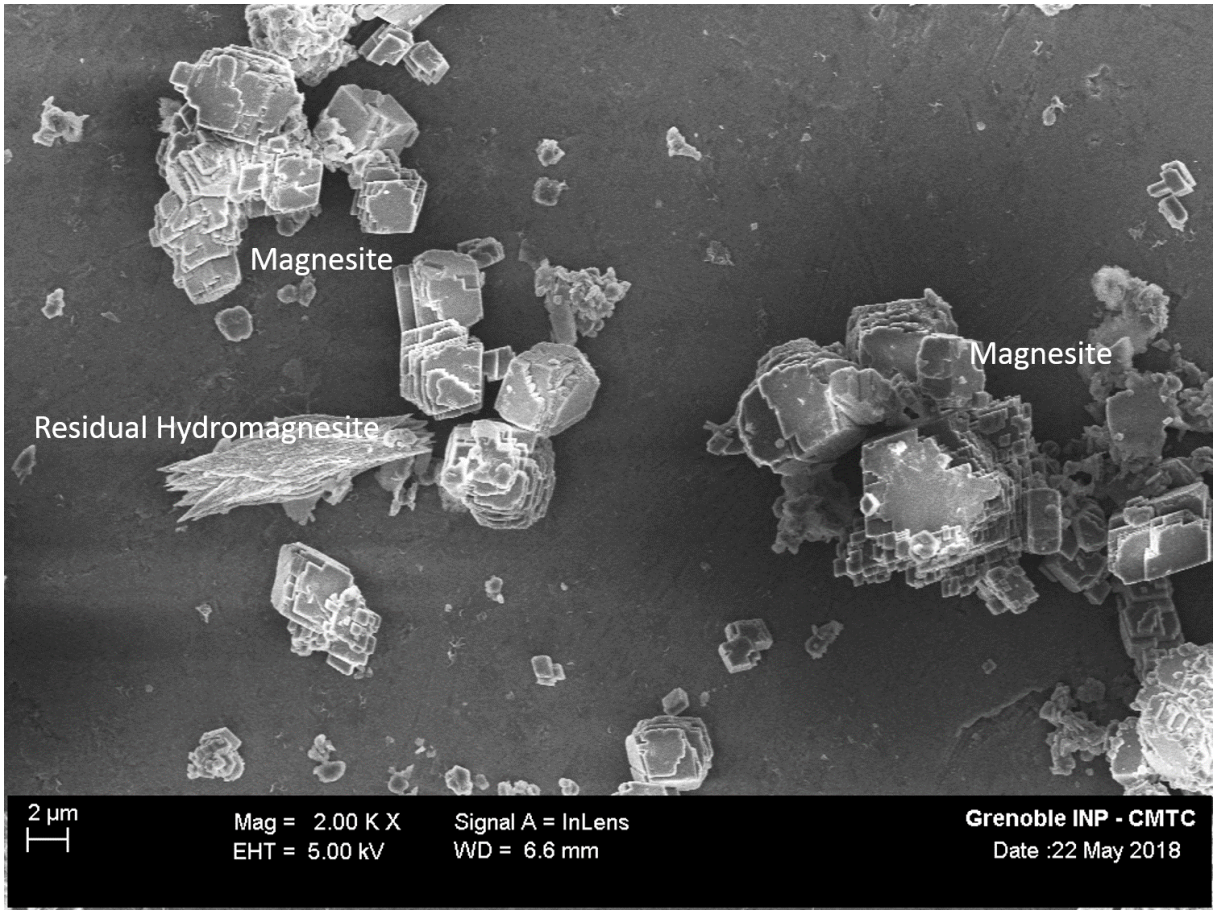

Figure SI-3 Field-emission gun scanning electron microscopy image of residual hydromagnesite and rhombohedral magnesite crystals with micrometer size (<5µm) produced after 24h at 90°C (run 3 in Table 1).

438

439

440

441

442

443

444

445

446

447

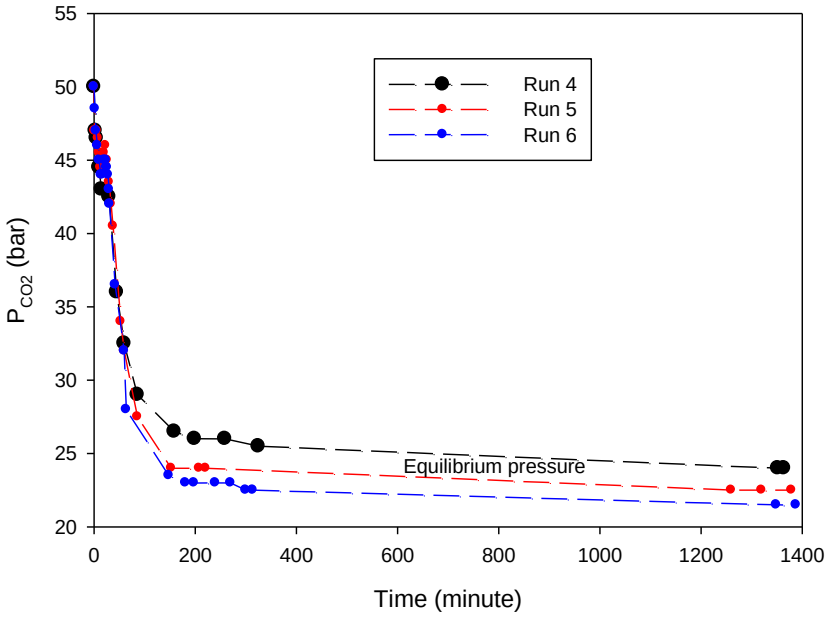

448

449

450 Figure SI-4. CO_2 pressure evolution during carbonation experiments at 60°C (runs 4 to 6 in Table
451 1).

452

453

454

455

456

457

458

459

460

461

462

463

464

465

466

467

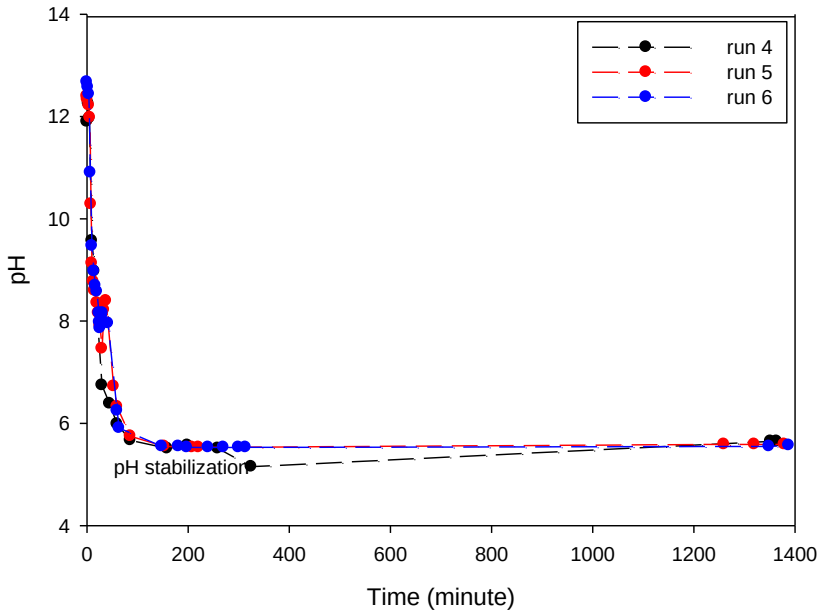

468

469

Figure SI-5. pH evolution as a function of time during carbonation experiments at 60°C (runs 4-6 in Table 1).